Landslides (2024) 21:529–540
DOI 10.1007/s10346-023-02185-6
Received: 16 August 2023
Accepted: 22 November 2023
Published online: 30 December 2023

Lucia Macías · María Quiñonez-Macías · Theofilos Toulkeridis · José Luis Pastor

Characterization and geophysical evaluation of the recent 2023 Alausí landslide in the northern Andes of Ecuador

Abstract The province of Chimborazo located in the northern Andes of Ecuador presents many intrinsic factors, which contribute to the occurrence of mass movements, leaving in many of the cases registered damages of materials and loss of life. The recent landslide of March 26, 2023, in the Alausí canton is an event of great interest due to the magnitude of the occurred destruction and the corresponding fatalities. Therefore, there are two predominant objectives of the current study, of which the first has been to determine the most relevant characteristics of this mass movement by identifying and analyzing the geomorphology of the recorded slope movement and the lithological units involved, by field work and through geophysical surveys. Secondly, we performed a preliminary study of the possible triggers of the movement by means of the historical analysis of the precipitations during the months of January to March of the last decade and the study of the recent seismic series. However, through the obtained analysis, it is determined that the study site is composed of three distinctive lithological units. The observed mass movement is of the rotational type, as result of the intense rainfall that occurred during the first quarter of 2023, being hereby the most probable triggering factor. This corresponds to a 600% increase in the average monthly rainfall compared to the period from 2010 to 2022.

Keywords Saturation · Precipitation · Rupture zone · Alausí landslide · Ecuador

Introduction

Environmental disasters indicate an increasing trend in terms of frequency and magnitude, and, above all, of human losses (Jonkman 2005; Petley et al. 2005; Auker et al. 2013; Pollock and Wartman 2020; Zhang et al. 2020). Developing countries are considered to be the regions with the greatest magnitude of natural disasters and therefore the largest affected populations, considering that these effects are amplified by human activities (Aristizábal and Sánchez 2020; Lacroix et al. 2020; Zhang et al. 2021; Panwar and Sen 2019; Du et al. 2010; Rubin and Rossing 2012; Petley 2012). Various natural disasters increase in their destructive power due to the current climate change playing a decisive role in recent times (Fang et al. 2019; Kundzewicz et al. 2014; Chen et al. 2020; Benevolenza and DeRigne 2019; Toulkeridis et al. 2020; Cappelli et al. 2021). Thus, globally, economic losses and fatalities from landslides are large and apparently rise over time (Sim et al. 2022; Gómez et al. 2023; Schuster and Fleming 1986). In many cases, this is due to the increase and expansion of settlements in dangerous areas of high vulnerability or inappropriate land use due to the lack of territorial planning (Soltani et al. 2019; Jiang et al. 2021; Santangelo et al. 2023).

Latin America in general and the Andean region specifically has had a large number of mass removals due to its varied morphology, geographic location, and geodynamic constellation as a result of an active plate margin in conjunction with the interference of various hydrometeorological processes and associated destructive phenomena such as La Niña and El Niño, also known as ENSO (Martinod et al. 2020; Sobolev and Babeyko 2005; Thielen et al. 2023). Thus, in Colombia, a total of 32,022 landslides have been registered between 1900 and 2016, produced by various causes, the most triggering factor is rain with 92%, reaching a very high level of risk (Garcia-Delgado et al. 2022). Similar increases have been registered in all the other Andean countries, including Ecuador, where the cause of deaths caused by natural disasters is led by mass removals (Miele et al. 2021; Sellers et al. 2021; Vallejo et al. 2018). Ecuador is situated in the interplay of the convergence of the Nazca oceanic plate with the South American and Caribbean continental plates, which results to the uprise of the Andean mountains, active volcanism, and geological faults as well as a high probability of landslide occurrence (Orejuela and Toulkeridis 2020; Poma et al. 2021). Landslides in this region occur due to the high elevations and associated strong dips of their slopes (Wilcke et al. 2003; Bravo-López et al. 2022; Puente-Sotomayor et al. 2021). Vulnerabilities are increased due to severe rainfall conditions which are demonstrated in the form of torrential and prolonged rains (Bathurst et al. 2010; Brenning et al. 2015; Tibaldi et al. 1995). Thus, the climatic conditions and the seismic events that hit the Andean region worsen the stability of slopes, becoming considered one of the regions with the greatest movements of deadly masses (Castelo et al. 2018).

Hereby, in Ecuador, the most fatal landslides within this mountain range are those that occurred in La Josefina (province of Azuay) in March 1993 (Harden 2001; Plaza et al. 2010), Gulag-Marianza (Cuenca) in March 2022, and the most recent in Alausí of March 2023 (Bravo-López et al. 2023). A condition of increased vulnerability to landslides occurs for social reasons (Kjekstad and Highland 2009; Wijaya and Hong 2018; Guillard-Gonçalves and Zêzere 2018). In the Andean cities, significant population growth has been evidenced, creating the need for new spaces for urban development, which subsequently cause an increase in deforestation and the use of slopes as construction land (Soto et al. 2017). Therefore, in the Chimborazo province, which is located in the Andean part of Ecuador, landslides have forced a change in the route of the highway in Alausí, Chunchi, Guamote, and Pallatanga (Bravo-López et al. 2023). Due to the existing circumstances, on March 26, 2023, in the Alausí canton, a rotational landslide occurred on an old landslide mass. This event occurred for some 50 s, leaving dozens fatalities, several

missing, and a great economic impact (Petley 2023). According to the classification proposed by Cruden and Varnes (1996), the movement is considered "extremely fast" and it took place in three phases.

Based on the aforementioned, the first analysis will allow the recognition of the geological features through the outcrop stratigraphy in the scarps, delimiting the rupture zone, secondary scarps, and accumulation of materials. Subsequently, through indirect methods, it is intended to obtain physical parameters of the study area, allowing the generation of models of the lithological units. Therefore, the present investigation aims predominantly to demonstrate the most relevant characteristics of this recent mass movement, through the identification and analysis of the lithological units studied from geophysical surveys, as well as the historical analysis of regional rainfall without discarding other possible causes such as those given by the seismic records.

Description of the study area

The Alausí canton is located in the province of Chimborazo, situated in the central region of the Andes of Ecuador, also known as the Sultana of the Andes, due to its proximity to majestic reliefs of prominent volcanoes (Fig. 1) (Coltorti and Ollier 2000; Mora et al. 2022). The city of Alausí has 42,823 inhabitants representing 10.6% of the total population of the province of Chimborazo (INEC 2001), counting with a young population (less than 20 years of age) that has a higher percentage of residences in rural areas. The main fluvial tributary is the Chanchan River, which rises from the mountainous foothills of Cruzpungo and crosses the Alausí Valley until it connects with the Chimbo River. In the study area of the observed landslide, the closest tributary is the Tingo stream that connects with the Chanchan River.

The slopes that surround the canton are part of paleolandslides that define the morphological instability of the area, with fractured, weathered materials and saturation caused by drainage systems and non-channeled water as a result of agricultural activity, which subsequently increases the probability of occurrence of mass movements (Aleksova et al. 2023). Lithologically, the recognition in the field at the Casual community site of Alausí allowed to present volcaniclastic sequences of the Cisarán geological formation, which is composed of andesites and basaltic andesites (Orbe et al. 2023; Williams et al. 2000). This andesitic basement is intruded by silicified whitish rhyolitic rocks, with sporadic quartz crystals, as evidenced in greater concentration on the right flank of the landslide, up to the Pueblo Viejo sector. On the crown of the landslide, there are laharitic deposits that contain homogeneous angular to subangular clasts. In the lahar horizons, debris avalanches have been identified in small areas on the crown and the southern flank of the landslide. Additionally, the so-called, widely distributed Cancagua formation is evidenced by brown-colored tuffs with conglomerate content, andesitic blocks, and subangular rhyolites with metric and centimeter sizes. In the lower parts of the study area, deposits of colluvial materials are observed whose matrix is poorly consolidated, with highly weathered and easily detachable blocks (Fig. 2).

Regarding the climatic characteristics of the study area, there is variability due to the diversity of ecological floors, presenting areas with a humid and temperate tropical climate, as well as

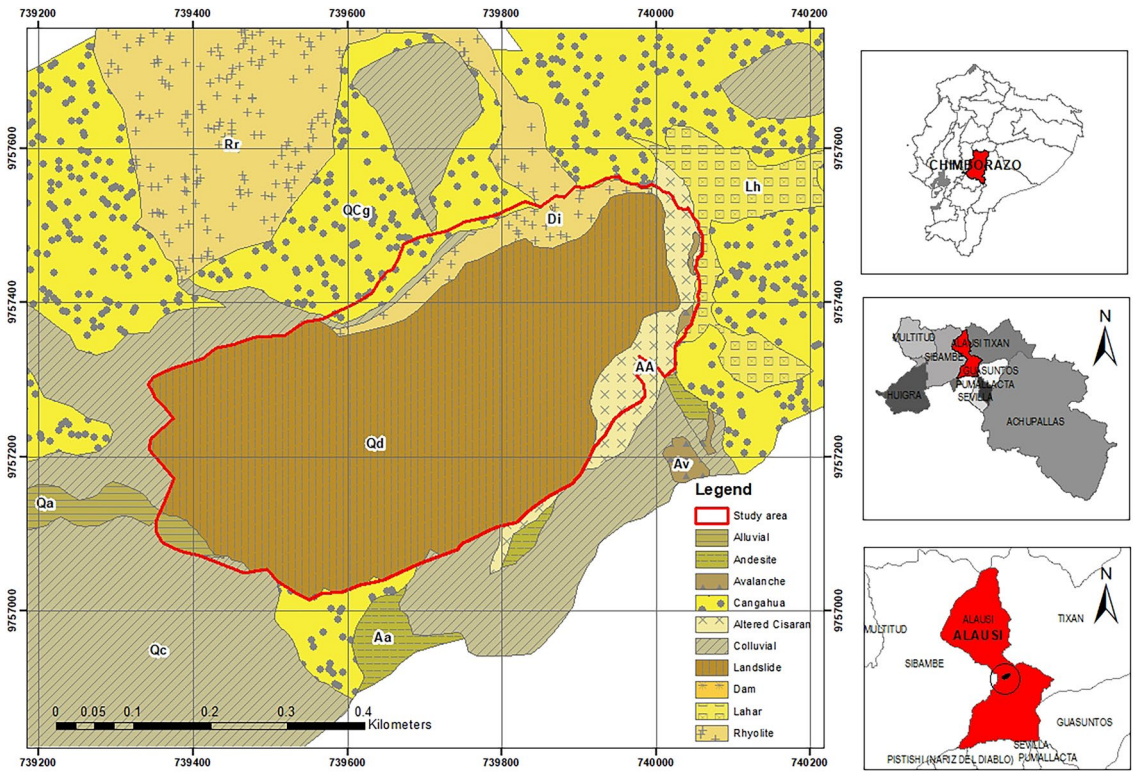

Fig. 1 Generalized geological map of the Alausí landslide, at coordinates 2°11′40.77″ S and 78°50′34.19″ W, modified from IIGE (IIGE 2023)

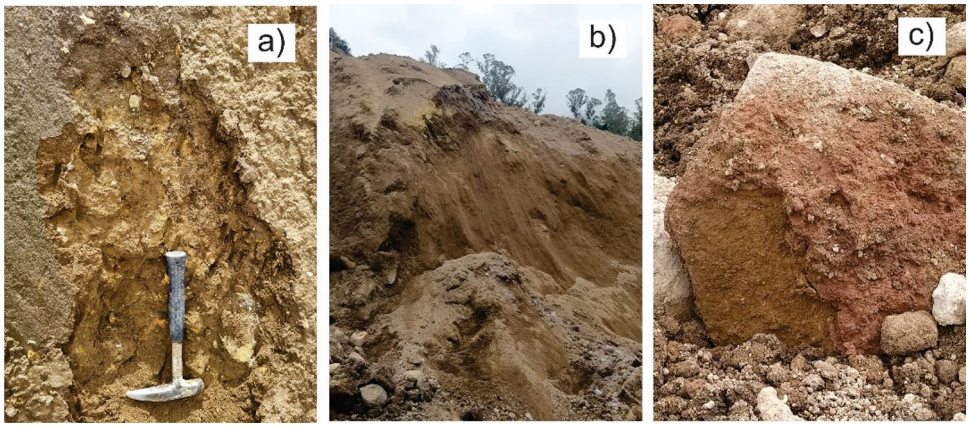

Fig. 2 Identified lithological units **a** volcanic rock blocks, **b** sandy silt and clayey silt consistency soils with gravel pebbles of rhyolitic igneous rock weathered to varying degrees, and **c** transported deposit with altered andesitic tuff fragments

sectors where the cold climate of the páramo predominates (Pilco 2013). The average annual temperature is 12 °C and annual rainfall varies between 250 and 500 mm, while the season with the highest humidity corresponds within the months of January and May (González-Ramírez et al. 2021).

Alausí is located on the Chaucha and Guamote lithotectonic complexes, which are composed of materials of continental and oceanic origin. At the regional level appears the Peltetec fault as well as the Pallatanga-Pujilí-Calacalí fault system, while locally crosses the Guamote-Alausí and Huigra-Guamote faults (Spikings et al. 2005; Alonso-Pandavenes et al. 2023; Aspden and Litherland 1992). Based on the NEC, being the Ecuadorian Construction Standard (Norma Ecuatoriana de la Construcción 2015), Alausí is located in the zone IV of the seismic hazard characterization, which is considered as high with a Z = 0.35. As specified in the catalog of the United States Geological Survey (USGS, 2023a), since 1964 the province of Chimborazo has registered more than three dozen seismic events with magnitudes greater than 3.8 and up to 5.6 M_w, from which a third of the registered earthquakes have had its focus or hypocenter located at depths less than or equal to 37 km. This allows to estimate that these events are probably of crustal origin and may be related to the faults identified in the study area. Seismicity and faults in the region increase the probability of landslides in the urban populations of Alausí, Tixán, Guasuntos, among others.

Methodology

After the occurrence of the landslide, we visited the area to gather information, collect data, and interview witnesses about the event. During the field activities, a preliminary evaluation of the main damages, affectations, and existing risks was realized. Through further observation and applying known methodologies (Bobrowsky and Couture 2014; Aspelin et al. 2009; Shanmugam and Wang 2015), the main characteristics of the landslide were determined. Additionally, activities conducted in the field have been the collection of topographic data using the DJI Matrice 300 RTK Multirotor drone, whose scope was to locate the coordinates of a station that serves as the basis for the real-time kinematic (RTK) link, allowing real-time correction (IIGE 2023). The processing of the aerial photography was performed using the Agisoft Metashape V1.4.3 build 6529 software, for the generation of orthomosaics, the digital surface model (DSM) and later to obtain the digital terrain model (DTM) that allowed to obtain the post-slide topography of Alausí. Finally, other topographic products such as orthophoto, a digital elevation model, and aerial photographs were obtained, which allowed obtaining detailed information about the landslide (Fig. 3).

Within the field work, geological and geophysical prospecting was realized, whose purpose has been to understand the lithological units and the stratigraphy of the study area (Lazcano 2012). For this purpose, shear wave velocity seismic tests (V_{s30}) were used, applying the ABEM brand equipment and the "Geogiga seismic Pro" software for field data processing. During the test, 24 geophones were used to identify the variation of shear waves with respect to depth. These data in units of measurement meters/second (m/s) were compared with the lithology evidenced on the ground in order to obtain a one-dimensional profile, through a mathematical inversion process for seismic data. The electrical tomography tests were generated using the ABEM Terrameter LS 3000 subsoil resistivity meter. The used electronic devices have been Wenner, Schlumberger as well as Gradient and 41 electrodes with a maximum current intensity of ± 600 V and 2500 mA, allowing the identification of the different subsoil strata and soil/rock lithological contacts.

Landslide characterization

The Alausí landslide of March 2023 is of the rotational type (Fig. 4), which, combined with the high saturation of the material, formed a subsequent debris flow. The landslide fragmented into a series of blocks, causing concentric and concave cracks in the direction of the displacement. Following the standardized criteria established by the UNESCO (1993), the landslide obtained a maximum width of the displaced mass of approximately 380 m, a depth of the displaced mass of 45 m, and the total length known as the distance from the crown up to the accumulation zone reaching up to 781 m in length (23.4 ha area) (Fig. 5). The crown of the slope is located at an elevation of 2586 m above sea level (m a.s.l.) and the foot of the slope at 2307 m a.s.l., obtaining a height of 279 m. The estimated volume of displaced material is approximately 125,000 m^3.

In the landslide, three well-differentiated deformation zones are able to be distinguished, delineated from topographic data

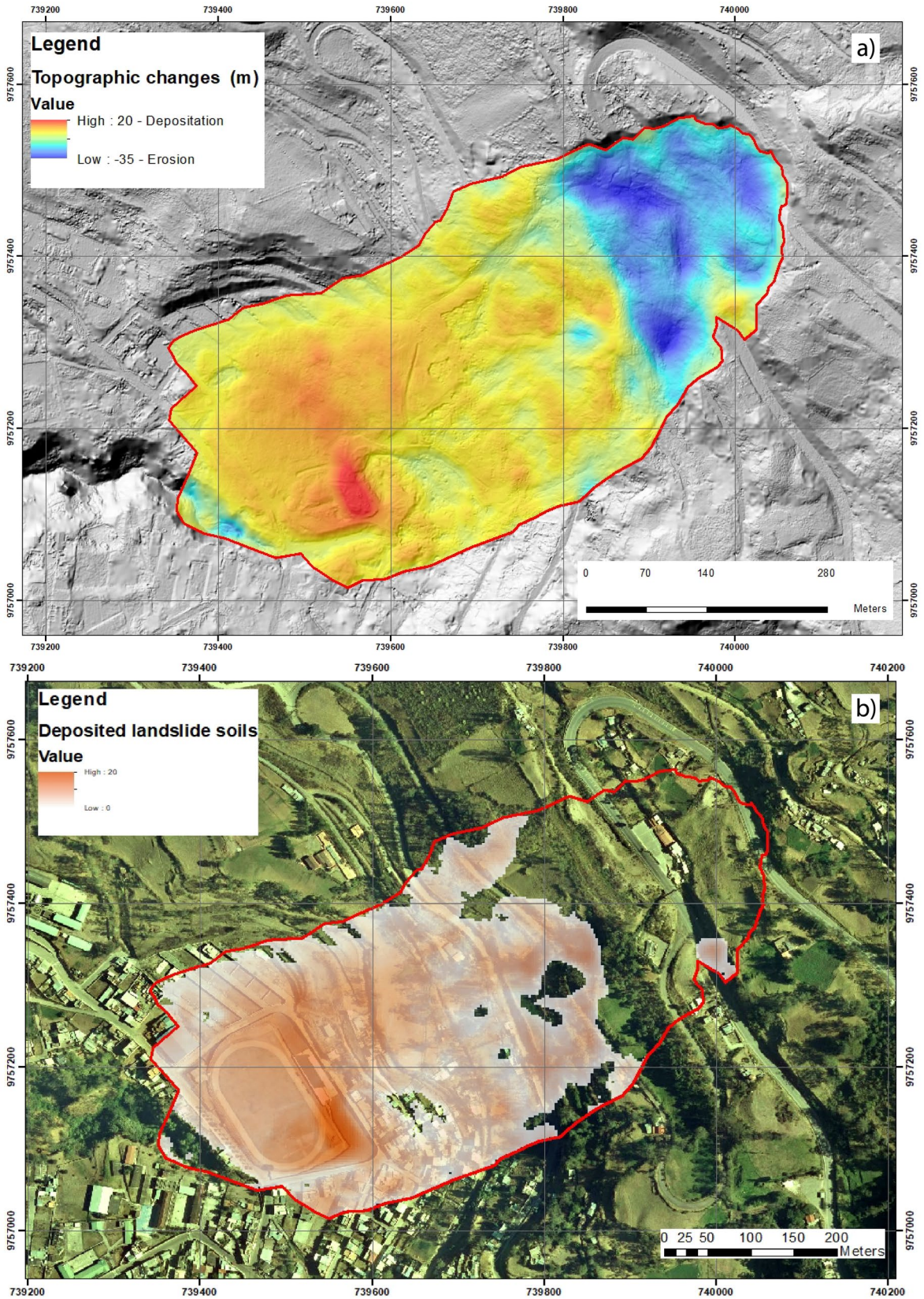

Fig. 3 Topographic changes. **a** Identification of the zone of erosion and deposition. **b** Zone of deposition

Fig. 4 Evidence of the Alausí landslide on March 26, 2023. **a** Rupture zone and rotational displacement. **b** Destroyed 1.2-km section of highway E35. **c** Quebrada el Tingo. **d** Main escarpment of the landslide with outcrops of three lithological units. **e** Homes and vehicles affected. **f** Total collapse of houses in the body of the landslide

and orthophotos, corresponding to three landslides that occurred consecutively (Fig. 6). In the first landslide that initiated at 9:13 p.m., it was possible to determine the presence of lahar-type material, composed of weathered rhyolitic igneous rock gravels and boulders also of volcanic origin, with angular shapes included in a sandy-silty matrix (SM), having a homogeneous structure and medium-dense compactness. The thicknesses range from 8 to 10 m, displaying a high level of saturation that resulted in a high speed of movement on the ground. The second landslide, which occurred some 10 min later, was the one with the highest deposition thickness in the accumulation zone, reaching up to 20 m of thickness. This corresponded to highly unstable materials due to their granulometric heterogeneity, resistance and low compaction, and with considerable levels of saturation. The third landslide corresponds to a series of debris flows, which covered a horizontal distance of approximately 300 m of displaced material, with thicknesses of 10 m near the secondary escarpments and 5 m in the final zone of the flow.

We identified the erosion zone with an approximate area of 66,000 m^2, representing 28% of the total affected area (Fig. 3a), while

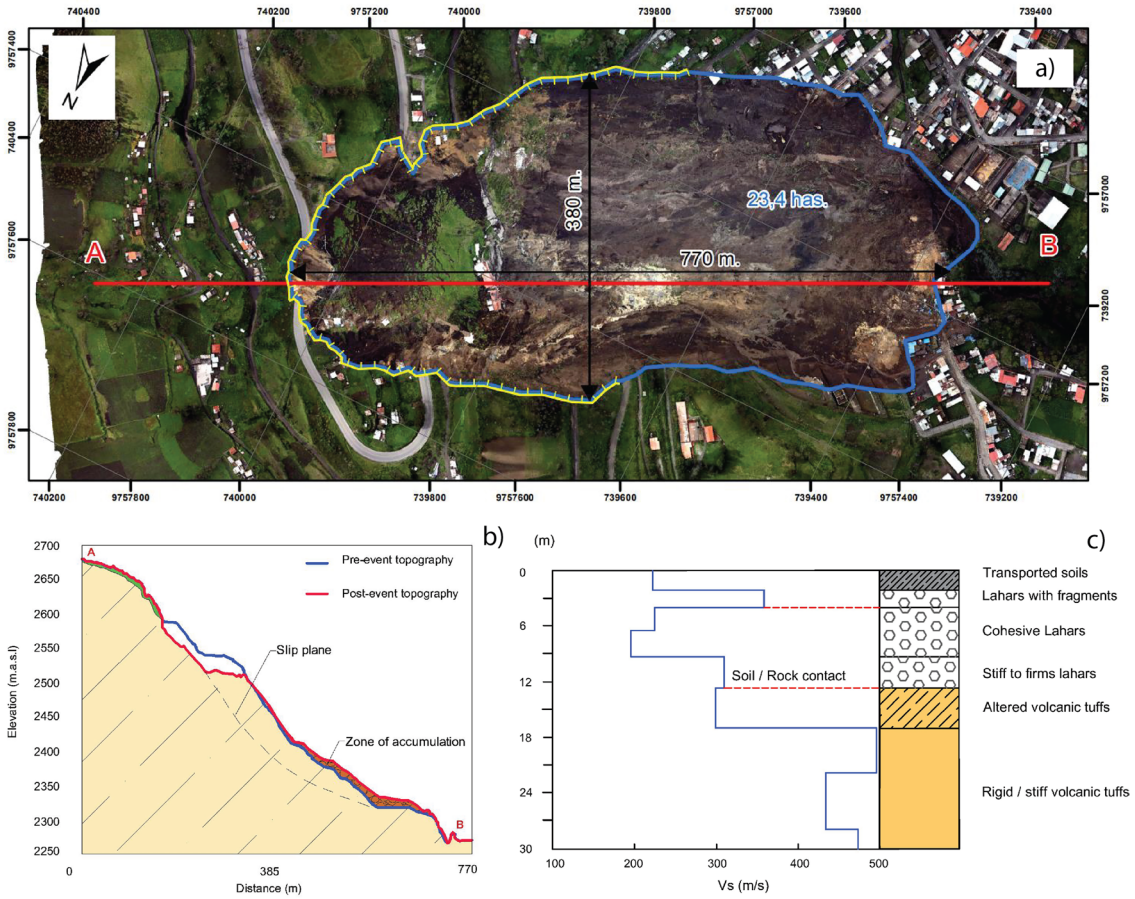

Fig. 5 Landslide topographic survey. **a** Plan view of the landslide. **b** Profile of the rotational type landslide. **c** Stratigraphic correlation with V_{s30} geophysical test data, before the landslide. This stratigraphic description has been collapsed with the slide of March 26, 2023 (SGR 2023)

the deposition zone reaches 166,000 m², which is equivalent to the residual 72%, with the largest deposit being located 600 m from the crown covering dozens of homes and recreational areas (stadium) (Fig. 3b) with deposit thicknesses that vary between 10 and 20 m. The main characteristics identified in the area of the event are the low cohesion of materials of silty sand consistency (SM) and low plasticity silt (ML), fractured, altered rocks and with various degrees of weathering that vary between II (slightly weathered) and IV (very weathered) according to the methods proposed by the ISRM (1981). In addition to having weaknesses between strata due to the intercalation of rigid and plastic materials, infiltration by non-channeled water from agricultural activity and septic tanks caused soil saturation, while the overload on the hillside is directly related to the construction of houses and road infrastructure.

In the observations realized after the slide, it was possible to demonstrate in the cuts of the escarpments and slopes, the well-differentiated stratigraphy of three lithological units, being (a) fine transported soils (colluvial) and secondary volcanic lahars with clasts and angular blocks of dacite or andesitic lavas, (b) fine-matrix volcanic lahars and sporadic andesite and tuff clasts, and (c) altered and rigid volcanic tuffs, corresponding to soil-rock contact, located between 13 and 18 m of depth. Figure 5 illustrates the limit between altered and bare rock.

The flows or mudslides caused by the macro landslide are products of the presence of sandy silty soils, clayey silts with gravel edges of weathered rhyolitic igneous rock, subjected to saturation conditions. In reference to the local geology, through the cuts of the escarpments formed on the site, the stratigraphy composed of microconglomerates and coarse sandstones of medium granulometry, with a sandy silt matrix, with rounded clasts of andesites, basalts, and diorites of millimeter to centimeters sizes is evident.

From the geophysical tests realized prior to the landslide, a record of seismic velocities was obtained that allowed the identification of the lithology of the study area. From the surface to 4 m, it presents $222 \leq V_s \leq 358$ m/s identified as fine transported soils (colluvial) and secondary volcanic lahars with clasts and angular blocks of dacite or andesitic lavas. Between 4 and 13 m with $196 \leq V_s \leq 310$ m/s recorded, it has been considered as fine-matrix volcanic lahars and sporadic clasts of andesites and tuffs. Finally, from 13 m wave speeds of $295 \leq V_s \leq 495$ are obtained, which are considered as altered volcanic tuffs and rigid, determining the soil/rock contact limit at a depth of 13 m. Based on the aforementioned data, a shear wave velocity at 30 m (V_{s30}) of 324 m/s is determined, which corresponds to a type of soil profile "D" for the study area according to the Ecuadorian Construction Standard (Norma Ecuatoriana de la Construcción 2015).

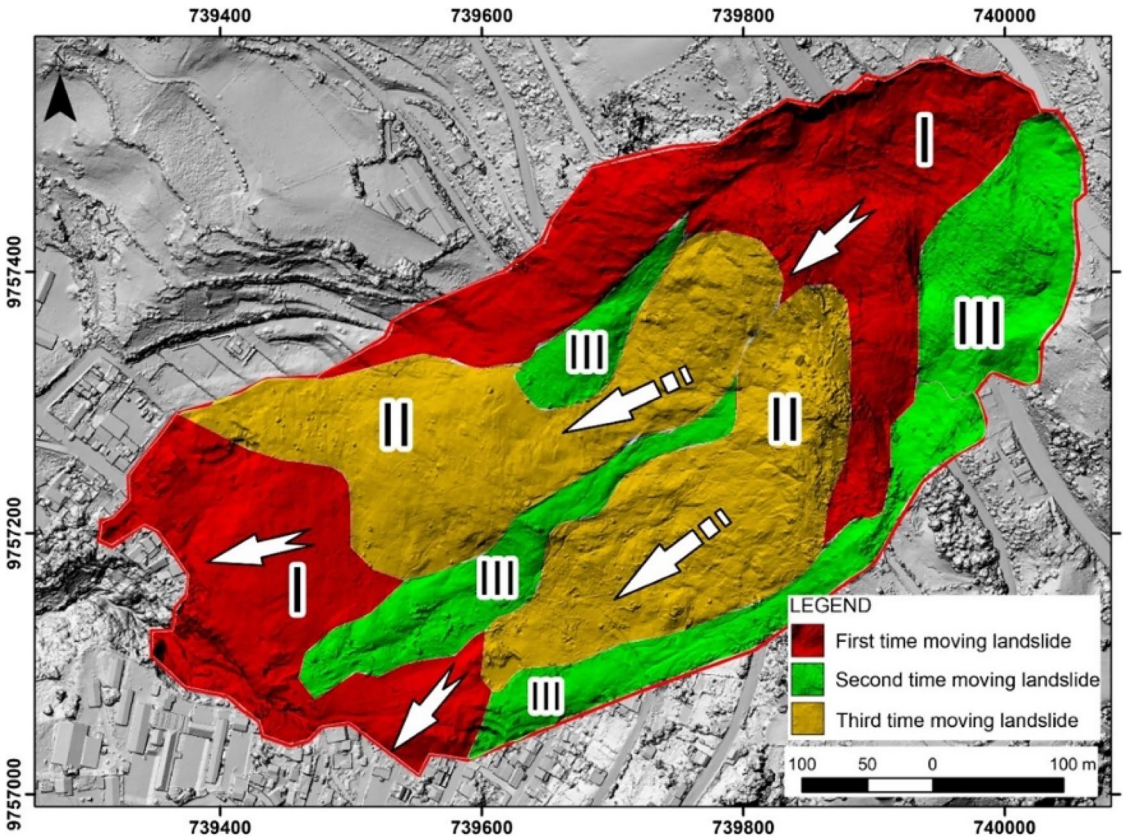

Fig. 6 Sequence of the landslide on March 26, 2023, in the city of Alausí

Months before the landslide, the deformation dynamics in the rocky substratum of the slope was evident, considering an active state due to the evidence of significant cracks in the study area. The corresponding dimensions were between 5 and 31 cm wide, depths of up to 2.7 m, and lengths of up to 21 m, as well as moderate to high levels of saturation due to poor use of water resources and abundant rainfall.

After the event, three seismic tests of shear wave velocity (V_{s30}) and three electrical tomography tests were performed in the body of the slide, allowing the identification of discontinuity and fracture systems, as well as saturation levels up to 20 m in depth (Fig. 7). In landslide 1, thicknesses between 8 and 10 m were observed, with resistivity values of 50 to 115 Ω·m (ohm·meter). This deformation dynamics present at the moment rigidity of the material. The measured velocities V_s are of the order of 550 to 750 m/s, due to the presence of andesitic blocks that were dragged during the slide (Fig. 2). Landslide 2 reached up to 20 m in thickness, and according to the realized electrical tomography, a channel area with considerable levels of saturation is evident. It is very probable that during the chaotic deposition of the landslide these channels with recorded values of 13 to 18 Ω·m were formed. The speeds V_s are in the order of 220 to 550 m/s. Finally, landslide 3 corresponds to debris flows with 10 m of thickness, with resistivity values of 24 to 84 Ω·m and V_s between 200 and 525 m/s. These are well differentiated in the terrain, while the consistency of the soil material varies by moisture content due to increased rainfall.

Preliminary evaluation of triggering factors

In order to obtain a preliminary estimate of the possible causes that could have triggered the landslide, the seismic events detected near Alausí in recent times, the precipitation data from a nearby meteorological station, and the collection of data may allow to recognize the most relevant characteristics of the study area. On March 18, 2023 (8 days prior the Alausí landslide), an earthquake with a magnitude of 6.8 (M_w) occurred near the city of Balao, of which epicenter has been located 130 km to the NE of the town of Alausí and at an depth of approximately 68 km (USGS 2023b) The epicentral intensity (I_o) assigned to the population of Alausí is IV according to the ESI (environment seismic intensity) scale (Michetti et al. 2007), since there is no evidence of fault ruptures (primary effects), with a correlatable assignment of seismic acceleration of 0.014 to 0.039 g (Wald et al. 2015). Therefore, the low seismic acceleration produced by the mentioned seismic movement in the study area rules out the seismic trigger as a precursor of the landslide.

Rainfall data from the Tixan weather station, located 7.5 km from the Alausí landslide site, have also been analyzed. Additionally, in the analysis of rainfall distribution, the data viewer of the National Aeronautics and Space Administration of the USA (NASA) was used, which contains information related to meteorological parameters to evaluate and design systems that use the renewable resource. The data recorded in the months of January to March, from 2010 to 2022, indicate average values from 56 to 238 mm, while in 2023 the values increased six times

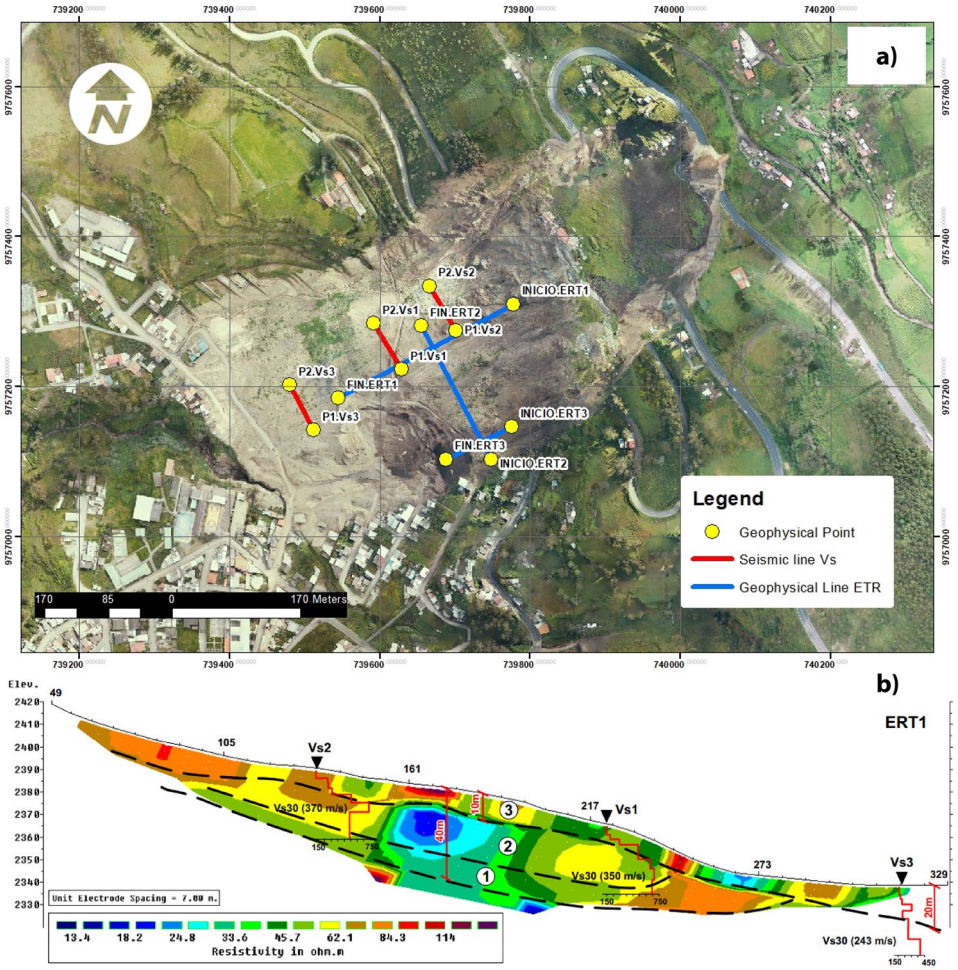

Fig. 7 **a** Location of lines for seismic tests V_{s30} and electrical tomography. **b** Geoseismic section in the Alausí landslide zone

the monthly average from 2010 to 2022, with ranges that vary monthly between the 699 to 1224 mm (see Fig. 8). These data were obtained from NASA as the Tixan weather station unfortunately lacked to be functional in the time period of interest.

The combination of different conditioning factors such as the low resistance of the materials and the topography of the slope together with the triggering effect of an accumulated rain, in the 3 months prior to the event, of six times the average of the last years, which seems to be the most probable cause of the recent rotational landslide observed in Alausí. More detailed investigation should be realized in order to understand the mechanism and causes of the landslide, as well as the susceptibility of the slope to further, new landslides.

Social and economic impacts

The studied landslide is located to the northeast of the urban area of Alausí, Casual sector, where the landslide and accumulation zone affected the land of 23 ha, with direct damage to the districts La Esperanza, Nuevo Alausí, Pircapamba, and Bua. According to the Secretary for Risk Management, the landslide left at least 75 people dead, 57 houses destroyed, and 581 people affected. Furthermore, there is significant damage to first and second order roads with an approximate length of 2.32 km, the collapse of 427 m of railway line, as well as affectation of at least 25% of the electrical network. Furthermore, there has been damage of some 60% of the drinking water service due to damage to 300 m of pipes and some less destruction of a school (Fig. 4). Part of the affected area involves the total loss of approximately six agricultural hectares with various crops (Secretaría de Gestión de Riesgo 2023). As a result of the landslide and the evidence of vulnerability in sectors surrounding the movement, many citizens were evacuated and housed in temporary sites. In addition to the human losses, material damage, and economic impact, the psychological impact and the feeling of insecurity generated in the inhabitants of the study site are part of the impact caused by this large landslide.

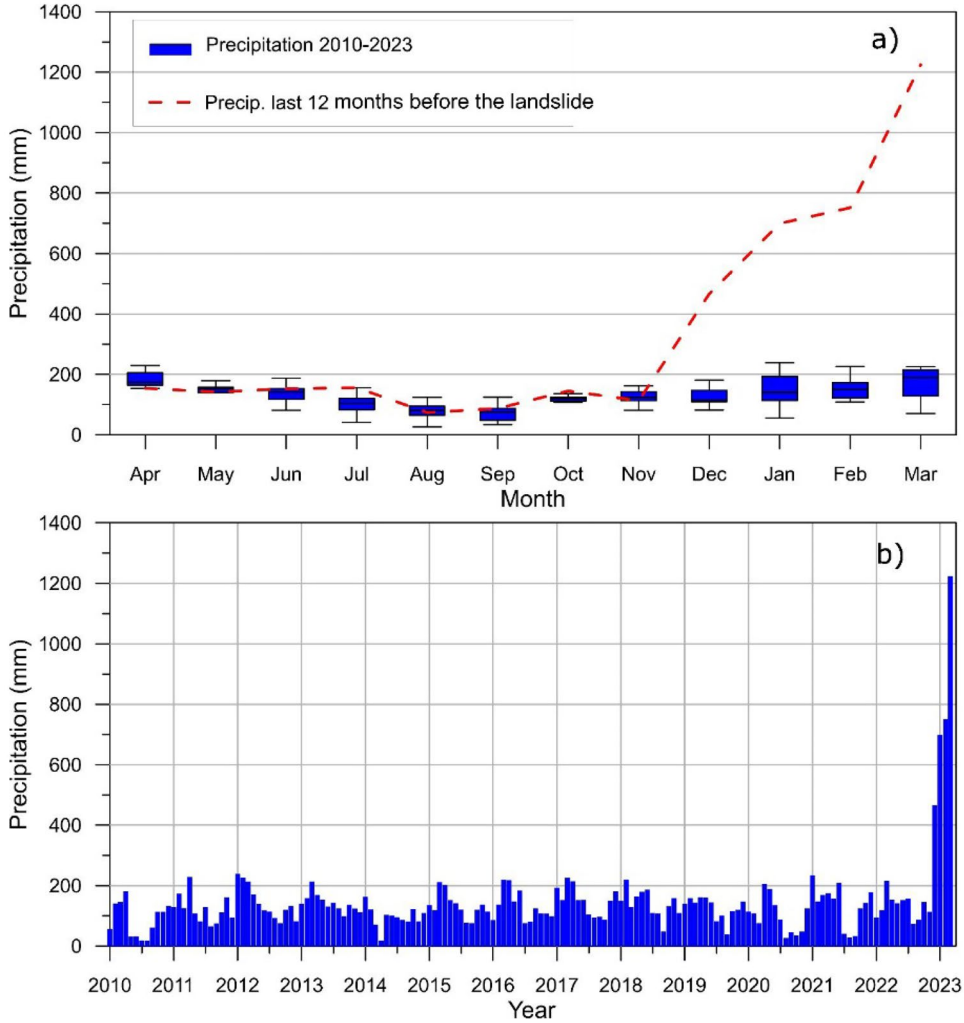

Fig. 8 **a** Box-and-whisker plot of monthly historical rainfall recorded in Alausí, with overlay of the last few months before the landslide. **b** Monthly precipitation recorded in Alausí between 2010 and 2023 (NASA 2023)

Conclusions

The landslide that occurred in Alausí on March 26, 2023, was of a rotational type, with the materials affected being fine transported soils (colluvial), volcanic lahars with a fine matrix and altered volcanic tuffs, corresponding to a type of soil profile "D".

There are several determining factors of the study site. Hereby, the topography of the hillside stands out, which presents a rugged relief in the form of mounds, depressions, and abrupt changes, which is the product of ancient mass movements, considering that Alausí is located in an area of active paleoslides.

The low cohesion of the materials together with the triggering effect of accumulated rainfall in the 3 months prior to the landslide that reached up to 600% of the average values of recent years seem to be the most probable cause of the observed landslide movement. A seismic trigger based on a previous strong earthquake is excluded to have been responsible for the fatal Alausí landslide.

Nonetheless, it will be necessary to conduct a more detailed investigation in order to fully understand the mechanism and causes of the landslide, as well as the susceptibility of the slope to future new landslides.

Acknowledgements

Thanks are extended to the public and authorities of Alausí during field studies. We thank further Kervin Chunga for his cooperation during fieldwork.

Funding Open Access funding provided thanks to the CRUE-CSIC agreement with Springer Nature.

Data availability

Not applied.

Declarations

Competing interests The authors declare no competing interests.

References

Aleksova B, Lukić T, Milevski I, Spalević V, Marković SB (2023) Modelling water erosion and mass movements (wet) by using GIS-based multi-hazard susceptibility assessment approaches: a case study—Kratovska Reka Catchment (North Macedonia). Atmosphere 14(7):1139. https://doi.org/10.3390/atmos14071139

Alonso-Pandavenes O, Bernal D, Torrijo FJ, Garzón-Roca J (2023) A comparative analysis for defining the sliding surface and internal structure in an active landslide using the HVSR passive geophysical technique in Pujilí (Cotopaxi). Ecuador Land 12(5):961. https://doi.org/10.3390/land12050961

Aristizábal E, Sánchez O (2020) Spatial and temporal patterns and the socioeconomic impacts of landslides in the tropical and mountainous Colombian Andes. Disasters 44(3):596–618. https://doi.org/10.1111/disa.12291

Aspden JA, Litherland M (1992) The geology and Mesozoic collisional history of the Cordillera Real. Ecuador Tectonophysics 205(1–3):187–204. https://doi.org/10.1016/0040-1951(92)90426-7

Aspelin P, Bellin MF, Jakobsen JÅ, Webb JAW (2009) Classification and terminology. Contrast Media 3–9. https://doi.org/10.1007/978-3-540-72784-2_1

Auker MR, Sparks RSJ, Siebert L, Crosweller HS, Ewert J (2013) A statistical analysis of the global historical volcanic fatalities record. J Appl Volcanol 2(1):1–24. https://doi.org/10.1186/2191-5040-2-2

Bathurst JC, Bovolo CI, Cisneros F (2010) Modelling the effect of forest cover on shallow landslides at the river basin scale. Ecol Eng 36(3):317–327. https://doi.org/10.1016/j.ecoleng.2009.05.001

Benevolenza MA, DeRigne L (2019) The impact of climate change and natural disasters on vulnerable populations: a systematic review of literature. J Hum Behav Soc Environ 29(2):266–281. https://doi.org/10.1080/10911359.2018.1527739

Bobrowsky P, Couture R (2014) Landslide terminology, Canadian technical guidelines and best practices related to landslides: a national initiative for loss reduction. Geological Survey of Canada, July. https://doi.org/10.4095/293940

Bravo-López E, Fernández Del Castillo T, Sellers C, Delgado-García J (2022) Landslide susceptibility mapping of landslides with artificial neural networks: multi-approach analysis of backpropagation algorithm applying the Neuralnet package in Cuenca. Ecuador Remote Sens 14(14):3495. https://doi.org/10.3390/rs14143495

Bravo-López E, Fernández Del Castillo T, Sellers C, Delgado-García J (2023) Analysis of conditioning factors in Cuenca, Ecuador, for landslide susceptibility maps generation employing machine learning methods. Land 12(6):1135. https://doi.org/10.4135/9781071873120.n8

Brenning A, Schwinn M, Ruiz-Páez AP, Muenchow J (2015) Landslide susceptibility near highways is increased by 1 order of magnitude in the Andes of southern Ecuador, Loja province. Nat Hazard 15(1):45–57. https://doi.org/10.5194/nhess-15-45-2015

Cappelli F, Costantini V, Consoli D (2021) The trap of climate change-induced "natural" disasters and inequality. Glob Environ Change 70(December 2020):102329. https://doi.org/10.1016/j.gloenvcha.2021.102329

Castelo CAJ, Dahowitt MC, Almeida OP, Toulkeridis T (2018) Comparative determination of the probability of landslide ocurrences and susceptibility in central Quito, Ecuador. 5th Int Conf EDemocracy EGovern, ICEDEG 2018:136–143. https://doi.org/10.1109/ICEDEG.2018.8372341

Chen S, Bagrodia R, Pfeffer CC, Meli L, Bonanno GA (2020) Anxiety and resilience in the face of natural disasters associated with climate change: a review and methodological critique. J Anxiety Disord 76:102297. https://doi.org/10.1016/j.janxdis.2020.102297

Coltorti M, Ollier C (2000) Geomorphic and tectonic evolution of the Ecuadorian Andes. Geomorphology 32(1–2):1–19. https://doi.org/10.1016/S0169-555X(99)00036-7

Cruden DM, Varnes DJ (1996) Landslide types and processes (pp. 36–75). Tuner, A.K Schuster R.L. (eds) Landslides: investigation and mitigation (special report)

Du W, FitzGerald GJ, Clark M, Hou XY (2010) Health impacts of floods. Prehosp Disaster Med 25(3):265–272

Fang J, Lau CKM, Lu Z, Wu W, Zhu L (2019) Natural disasters, climate change, and their impact on inclusive wealth in G20 countries. Environ Sci Pollut Res 26(2):1455–1463. https://doi.org/10.1007/s11356-018-3634-2

Garcia-Delgado H, Petley DN, Bermúdez MA, Sepúlveda SA (2022) Fatal landslides in Colombia (from historical times to 2020) and their socio-economic impacts. Landslides 19(7):1689–1716

Gómez D, García EF, Aristizábal E (2023) Spatial and temporal landslide distributions using global and open landslide databases. Nat Hazards 117(1):25–55. https://doi.org/10.1007/s11069-023-05848-8

González-Ramírez LC, Vázquez CJ, Chimbaina MB, Djabayan-Djibeyan P, Prato-Moreno JG, Trelis M, Fuentes MV (2021) Ocurrence of enteroparasites with zoonotic potential in animals of the rural area of San Andres, Chimborazo, Ecuador. Veterinary Parasitology: Regional Studies and Reports 26:100630. https://doi.org/10.1016/j.vprsr.2021.100630

Guillard-Gonçalves C, Zêzere JL (2018) Combining social vulnerability and physical vulnerability to analyse landslide risk at the municipal scale. Geosciences 8(8):294. https://doi.org/10.3390/geosciences8080294

Harden C (2001) Sediment movement and catastrophic events: the 1993 rockslide at la Josefina. Ecuador Physical Geography 22(4):305–320. https://doi.org/10.1080/02723646.2001.10642745

IIGE (2023) Levantamiento de informacion de campo y consideraciones geologicas en el deslizamiento ocurrido el 29 de marzo de 2023 en Alausi porvincia de Chimborazo, Ecuador

INEC (2001) Instituto Nacional de Estadística y Censos. https://www.ecuadorencifras.gob.ec/institucional/home/

ISRM (1981) Rock characterization, testing & monitoring: ISRM suggested methods. International Society for Rock Mechanics, Commission on Testing Methods

Jiang S, Meng J, Zhu L, Cheng H (2021) Spatial-temporal pattern of land use conflict in China and its multilevel driving mechanisms. Sci Total Environ 801:149697. https://doi.org/10.1016/j.scitotenv.2021.149697

Jonkman SN (2005) Global perspectives on loss of human life caused by floods. Nat Hazards 34(2):151–175. https://doi.org/10.1007/s11069-004-8891-3

Kjekstad O, Highland L (2009) Economic and social impacts of landslides. Landslides–Disaster Risk Reduction 573–587

Kundzewicz ZW, Kanae S, Seneviratne SI, Handmer J, Nicholls N, Peduzzi P, Mechler R, Bouwer LM, Arnell N, Mach K, Muir-Wood R, Brakenridge GR, Kron W, Benito G, Honda Y, Takahashi K, Sherstyukov B (2014) Flood risk and climate change: global and regional perspectives. Hydrol Sci J 59(1):1–28. https://doi.org/10.1080/02626667.2013.857411

Lacroix P, Handwerger AL, Bièvre G (2020) Life and death of slow-moving landslides. Nat Rev Earth Environ 1(8):404–419. https://doi.org/10.1038/s43017-020-0072-8

Lazcano S (2012) Perfiles de velocidad de onda de corte y análisis del comportamiento sísmico del suelo en el poniente de Guadalajara, Jal. XXVI Reunión Nacional de Mecánica de Suelos e Ingeniería Geotécnica 1–8. https://www.researchgate.net/publication/343588532_Perfiles_de_velocidad_de_onda_de_corte_y_analisis_del_comportamiento_sismico_del_suelo_en_el_poniente_de_Guadalajara_Jal_Mexico_Shear_wave_profiles_and_soil_seismic_behavior_in_the_West_part_of_Guadal

Martinod J, Gérault M, Husson L, Regard V (2020) Widening of the Andes: an interplay between subduction dynamics and crustal wedge tectonics. Earth Sci Rev 204:103170. https://doi.org/10.1016/j.earscirev.2020.103170
Michetti AM, Esposito E, Guerrieri L, Porfido S, Serva L, Tatevossian R, Roghozin E (2007) Environmental seismic intensity scale-ESI 2007. Memorie Descrittive Della Carta Geologica d'Italia 74(1):7–23. http://www.isprambiente.gov.it/en/publications/technical-periodicals/descriptive-memories-of-the-geological-map-of/intensity-scale-esi-2007?set_language=en
Miele P, Di Napoli M, Guerriero L, Ramondini M, Sellers C, Annibali Corona M, Di Martire D (2021) Landslide awareness system (Laws) to increase the resilience and safety of transport infrastructure: the case study of pan-American highway (Cuenca–Ecuador). Remote Sens 13(8):1564. https://doi.org/10.3390/rs13081564
Mora MMJ, González CAL, Hidalgo DAE, Toulkeridis T (2022) Determination of altitudes of the three main Ecuadorian summits through GNSS positioning. Geod Geodyn 13(4):343–351. https://doi.org/10.1016/j.geog.2021.11.006
NASA (2023) Power/data access viewer. https://power.larc.nasa.gov/data-access-viewer/
Norma Ecuatoriana de la Construcción (2015) NEC-SE-DS Cargas Sísmicas Diseño Sismo Resistente. In Norma Ecuatoriana de la Construcción. http://www.indeci.gob.pe/proyecto58530/objetos/archivos/20110606102841.pdf/0A https://www.habitatyvivienda.gob.ec/wp-content/uploads/downloads/2015/02/NEC-SE-DS-Peligro-Sísmico-parte-1.pdf . in spanish
Orbe J, Herrera-Robalino JL, Ureña-Callay G, Telenchano-Ilbay J, Samaniego-León S, Fienco-Bacusoy A, Cando-Veintimilla A, Toulkeridis T (2023) An evaluation of radon in drinking water supplies in major cities of the province of Chimborazo, central Andes of Ecuador. Water 15(12):2255. https://doi.org/10.3390/w15122255
Orejuela IP, Toulkeridis T (2020) Evaluation of the susceptibility to landslides through diffuse logic and analytical hierarchy process (AHP) between Macas and Riobamba in Central Ecuador. In 2020 Seventh International Conference on eDemocracy and eGovernment, ICEDEG 2020, pp. 201–207. https://doi.org/10.1109/ICEDEG48599.2020.9096879
Panwar V, Sen S (2019) Economic impact of natural disasters: an empirical re-examination. Margin 13(1):109–139. https://doi.org/10.1177/0973801018800087
Petley D, Dunning SA, Rosser NJ (2005) The analysis of global landslide risk through the creation of a database of worldwide landslide fatalities. In Landslide Risk Management, pp. 377–384. CRC Press
Petley D (2023) Alausí: a massive landslide in Ecuador. https://blogs.agu.org/landslideblog/2023/03/28/alausi-1/
Petley D (2012) Global patterns of loss of life from landslides. Geology 40(10):927–930. https://doi.org/10.1130/G33217.1
Pilco J (2013) Propuesta estratégica de marketing para la difusión, comercialización y fortalecimiento de los principales atractivos turísticos del cantón Alausí para el periodo 2013–2014. [Universidad Superior Politécnica de Chimborazon]. In Pontificia Universidad Catolica del Peru. http://dspace.espoch.edu.ec/bitstream/123456789/6237/1/42T00330.pdf
Plaza G, Zevallos O, Cadier É (2010) La Josefina landslide dam and its catastrophic breaching in the Andean region of Ecuador. Natural and Artificial Rockslide Dams, 389–406. https://doi.org/10.1007/978-3-642-04764-0_14
Pollock W, Wartman J (2020) Human Vulnerability to Landslides Geohealth 4(10):1–17. https://doi.org/10.1029/2020GH000287
Poma P, Usca M, Fdz-Polanco M, Garcia-Villacres A, Toulkeridis T (2021) Landslide and environmental risk from oil spill due to the rupture of SOTE and OCP pipelines, San Rafael Falls, Amazon Basin, Ecuador. Int J Adv Sci Eng Inf Technol 11(4):1558–1566. https://doi.org/10.18517/ijaseit.11.4.13727
Puente-Sotomayor F, Mustafa A, Teller J (2021) Landslide susceptibility mapping of urban areas: logistic regression and sensitivity analysis applied to Quito. Ecuador Geoenvironmental Disasters 8(1):19. https://doi.org/10.1186/s40677-021-00184-0
Rubin O, Rossing T (2012) National and local vulnerability to climate-related disasters in Latin America: the role of social asset-based adaptation. Bull Lat Am Res 31(1):19–35. https://doi.org/10.1111/j.1470-9856.2011.00607.x
Santangelo M, Althuwaynee O, Alvioli M, Ardizzone F, Bianchi C, Brunetti M, Bucci F, Cardinali M, Donnini M, Esposito G, Gariano SL, Grita S, Marchesini I, Melillo M, Peruccacci S, Salvati P, Yazdani M, Fiorucci F (2023) Inventory of landslides triggered by an extreme rainfall event in Marche-Umbria, Italy, on 15 September 2022. Sci Data 10(May). https://doi.org/10.1007/s10346-023-02109-4
Schuster RL, Fleming RW (1986) Economic losses and fatalities due to landslides. Bull Assoc Eng Geol 23(1):11–28. https://doi.org/10.2113/gseegeosci.xxiii.1.11
Sellers CA, Buján S, Miranda D (2021) MARLI: a mobile application for regional landslide inventories in Ecuador. Landslides 18(12):3963–3977. https://doi.org/10.1007/s10346-021-01764-9
SGR (2023) Informe Nº. SGR-IASR-08–2023–002
Shanmugam G, Wang Y (2015) The Landslide Problem Journal of Palaeogeography 4(2):109–166. https://doi.org/10.3724/SP.J.1261.2015.00071
Sim KB, Lee ML, Wong SY (2022) A review of landslide acceptable risk and tolerable risk. Geoenviron Disasters 9(1). https://doi.org/10.1186/s40677-022-00205-6
Secretaría de Gestión de Riesgo (2023) Deslizamiento Casual - Alausí (Issue 74)
Sobolev SV, Babeyko AY (2005) What drives orogeny in the Andes? Geology 33(8):617–620. https://doi.org/10.1130/G21557.1
Soltani A, Inaloo RB, Rezaei M, Shaer F, Riyabi MA (2019) Spatial analysis and urban land use planning emphasising hospital site selection: a case study of Isfahan city. Bulletin of Geography Socio-Economic Series 43(1):71–89. https://doi.org/10.2478/bog-2019-0005
Soto J, Galve JP, Palenzuela JA, Azañón JM, Tamay J, Irigaray C (2017) A multi-method approach for the characterization of landslides in an intramontane basin in the Andes (Loja, Ecuador). Landslides 14(6):1929–1947. https://doi.org/10.1007/s10346-017-0830-y
Spikings RA, Winkler W, Hughes RA, Handler R (2005) Thermochronology of allochthonous terranes in Ecuador: unravelling the accretionary and post-accretionary history of the Northern Andes. Tectonophysics 399(1–4):195–220. https://doi.org/10.1016/j.tecto.2004.12.023
Thielen DR, Ramoni-Perazzi P, Zamora-Ledezma E, Puche ML, Marquez M, Quintero JI, Rojas W, Quintero A, Bianchi G, Soto-Werschitz IA, Arizapana-Almonacid MA (2023) Effect of extreme El Niño events on the precipitation of Ecuador. Nat Hazards Earth Syst Sci 23(4):1507–1527. https://doi.org/10.5194/nhess-23-1507-2023
Toulkeridis T, Tamayo E, Simón-Baile D, Merizalde-Mora MJ, Reyes -Yunga DF, Viera-Torres M, Heredia M (2020) Climate change according to Ecuadorian academics-perceptions versus facts. Granja 31(1):21–49. https://doi.org/10.17163/lgr.n31.2020.02
Tibaldi A, Ferrari L, Pasquarè G (1995) Landslides triggered by earthquakes and their relations with faults and mountain slope geometry: an example from Ecuador. Geomorphology 11(3):215–226. https://doi.org/10.1016/0169-555X(94)00060-5
UNESCO Working Party on World Landslide Inventory (1993) Multilingual landslide glossary. BiTech Publishers British Columbia, Canada, Richmond
USGS (United States Geological Service) (2023a) Earthquake catalog search. https://earthquake.usgs.gov/earthquakes/search/
USGS (United States Geological Service) (2023b) M 6.8 - 14 km NNW of Baláo, Ecuador. https://earthquake.usgs.gov/earthquakes/eventpage/us7000jl3s/executive
Vallejo RZ, Almeida OP, D'Howitt MC, Toulkeridis T, Rodriguez F, Mato F, Munoz BM (2018) Numerical probability modeling of past, present and future landslide occurrences in nothern Quito, Ecuador. In 2018 International Conference on eDemocracy & eGovernment (ICEDEG) (pp. 117–125). IEEE. https://doi.org/10.1109/ICEDEG.2018.8372372

Wald DJ, Worden BC, Quitoriano V, Pankow KL (2015) ShakeMap manual: technical manual, user's guide, and software guide. U.S. Geological Survey, Techniques and Methods 12-A1, 132

Wijaya AP, Hong JH (2018) Quantitative assessment of social vulnerability for landslide disaster risk reduction using GIS approach (case study: Cilacap regency, province of central Java, Indonesia). International Archives of the Photogrammetry, Remote Sensing and Spatial Information Sciences 42:703–709. https://doi.org/10.5194/isprs-archives-XLII-4-703-2018

Wilcke W, Valladarez H, Stoyan R, Yasin S, Valarezo C, Zech W (2003) Soil properties on a chronosequence of landslides in montane rain forest. Ecuador Catena 53(1):79–95. https://doi.org/10.1016/S0341-8162(02)00196-0

Williams TM, Dunkley PN, Cruz E, Acitimbay V, Gaibor A, Lopez E, Baez N, Aspden JA (2000) Regional geochemical reconnaissance of the Cordillera Occidental of Ecuador: economic and environmental applications. Appl Geochem 15(4):531–550. https://doi.org/10.1016/S0883-2927(99)00059-1

Zhang F, Peng J, Huang X, Lan H (2021) Hazard assessment and mitigation of non-seismically fatal landslides in China. Nat Hazards 106(1):785–804. https://doi.org/10.1007/s11069-020-04491-x

Zhang S, Li C, Zhang L, Peng M, Zhan L, Xu Q (2020) Quantification of human vulnerability to earthquake-induced landslides using Bayesian network. Eng Geol 265:105436. https://doi.org/10.1016/j.enggeo.2019.105436

Lucia Macías (✉) · José Luis Pastor
Department of Civil Engineering, University of Alicante, P.O. Box 99, 03080 Alicante, Spain
Email: lucia.macias@utm.edu.ec

Lucia Macías
Department of Civil Construction, Faculty of Mathematical, Physical and Chemical Sciences, Technical University of Manabí (UTM), Av. José María Urbina, Portoviejo 130111, Ecuador

María Quiñonez-Macías
Secretariat of Risk Management (SGR), Integrated Security Center Building, Samborondón 092301, Ecuador

Theofilos Toulkeridis
Department of Earth and Construction Sciences, University of the Armed Forces ESPE, Sangolquí 171103, Ecuador